Microfluidic Minimum Inhibitory Concentration Test for Point-of-Care Assessment of Typhoid Fever

Kaycee Sapasap, Kishant Mohan, Shikha Kathrani

Abstract*—Antibiotic resistance is a growing health concern that delays effective treatment and contributes to increased mortality rates worldwide. Many cases of antibiotic resistance arise from overuse of antibiotics when appropriate dosing information is unavailable at the time of treatment. This study presents a microfluidic device that tests multiple antibiotic concentrations against S. Typhi isolated from a whole drop of blood to determine the minimum inhibitory concentration (MIC) for appropriate antibiotic dosing. In calculating the exponential growth rate of bacteria and selectively choosing the dimensions of our channels, our device achieves a readout time within 9 hours. Through the use of soft lithography techniques, reduced reagent usage, and minimal patient sample requirements, the results of this study revealed a potential point-of-care screening approach for determining appropriate antibiotic dosing. Further optimization in patient blood sample volume and sample injection methods may reduce assay time and cost, improving feasibility for point-of-care applications.

I. INTRODUCTION

Typhoid fever, an infection caused by Salmonella enterica serovar Typhi (*S. typhi*), remains a major global public health burden, with the Global Burden of Disease study estimating more than 7 million cases and 93,000 deaths worldwide in 2021 [1]. Typhoid disproportionately affects low and middle income countries in South Asia, Southeast Asia, and sub-Saharan Africa, where poverty, limited healthcare funding, and the lack of quality hospital and laboratory infrastructure delay diagnosis and treatment, making accessible point-of-care testing especially important [2]. Moreover, the disease presents with nonspecific symptoms that overlap with malaria, dengue, rickettsioses, leptospirosis, and melioidosis, making clinical diagnosis challenging and driving widespread empiric antibiotic treatment [3]. Decades of unregulated antibiotic use have led to the emergence of multidrug-resistant (MDR) and extensively drug-resistant (XDR) *Salmonella Typhi*, including the H58 lineage and the large XDR outbreak in Sindh, Pakistan between 2016 and 2018 [4]. As resistance to first-line antibiotics such as fluoroquinolones has become widespread, azithromycin has emerged as one of the few remaining oral treatment options for uncomplicated typhoid fever due to its high bioavailability and strong intracellular penetration. However, recent studies have reported increasing azithromycin resistance, particularly in Bangladesh, Nepal, India, and Pakistan, where mutations such as R717Q/L in the AcrB efflux pump reduce susceptibility, raising concerns about the reliability of this last-line oral therapy. [5, 6]

Diagnostic limitations further contribute to resistivity of azithromycin as long assay times results often result in clinicians administering higher doses of antibiotics to rapidly initiate rapid treatment. The current gold standard, blood culture, has low sensitivity and requires at least 7 days of observation before reporting a negative result [7, 8]. Other AST methods, like agar diffusion and broth microdilution, enable scientists to determine quantitative minimum inhibitory concentration (MIC), require bulk bacterial growth, requiring 16-24 hours of incubation to reach detectable optical density thresholds of (~10^7 CFU/mL), and must be performed in centralized laboratories, delaying therapy [9]. Microfluidic platforms are uniquely positioned to address this issue by enabling high-throughput testing at low sample volumes and short-time scales. Our device uses a Christmas-tree-style microfluidic gradient generator to expose bacteria to a set of discrete azithromycin concentrations arranged in a linear gradient. We do not use the standard two-fold dilution method common in broth microdilution studies. Instead, we selected azithromycin concentrations based on published clinical data showing the distribution of MICs for *S. Typhi*, where most isolates fall between 2 and 8 mg/L, susceptibility is defined as MIC $\leq$ 16 mg/L, and resistant is defined as MIC $\geq$ 32 mg/L. [6]. By choosing concentrations that span this range, our device is designed to appropriately distinguish between susceptible and resistant bacterial isolates while capturing a majority of clinically reported MIC values. The Christmas-tree design works by repeatedly splitting and recombining a stream composed of antibiotic, media, and fluorescent dye with another stream composed of no antibiotic, media, and fluorescent dye to create stable dilution ratios and a linear concentration gradient across the outlets. [10, 11]. Bacteria is then separated from whole blood in another stage of the device and loaded into these outlets. Incubation then follows, allowing fluorescent visualization of bacterial viability across concentrations and determination of MIC for appropriate antibiotic dosing. Because these concentrations are predefined, the results can be interpreted directly by observing bacterial growth, without requiring external calibration, sensors, or complex image analysis. Our selection of sample and reagent volumes and channel dimensions also allow for MIC readout within 9 hours. Additionally, the branching structure of the tree-gradient design makes it easy to later expand the platform to test multiple antibiotics on a single chip.

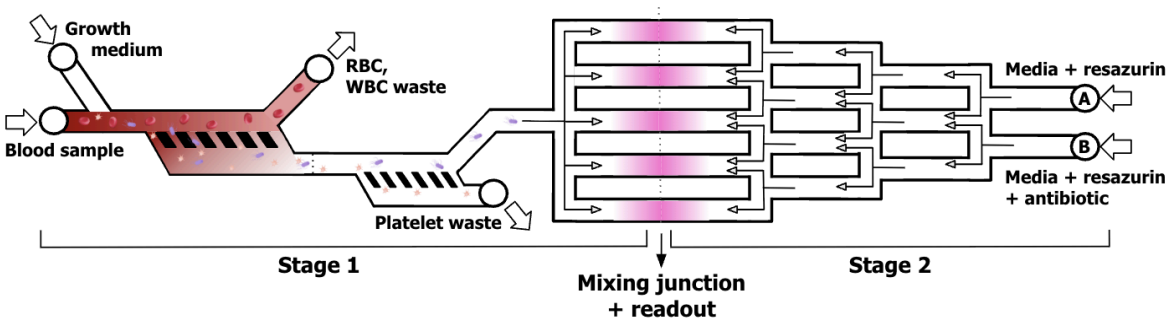

Figure 1: General layout of the device. Stage 1 filters bacteria from blood and is divided among 5 channels. Stage 2 is a Christmas Tree gradient generator that makes the appropriate antibiotic concentrations needed for MIC readout.

II. DEVICE DESCRIPTION

Our device is a two-stage PDMS microfluidic platform fabricated using soft lithography. The first stage is designed to isolate *S. Typhi* from blood and the second stage creates a concentration gradient of azithromycin for determination of MIC. In Stage 1, whole blood is injected into an inlet via syringe pump and enters a rectangular microchannel under pressure-driven laminar flow. Since the blood contains various components of different sizes, as seen in Table 1, there are two filters in stage 1 to appropriately separate *S. typhi* from RBCs, WBCs, and platelets [12, 13, 14]. The first filter has a pore size of 4 µm to allow for bacteria and platelets to fall through while keeping RBCs and WBCs above the filter and out to a waste channel. Depending on how the individual bacteria is oriented as it approaches a pore, it may not be able to pass through even if its width is small enough, so we recognize that some S. Typhi cells may be lost during filtration. The second filter then has a pore size of 3 µm to allow platelets to fall through and out to a waste channel while keeping the bacteria above the filter. This bacteria then leaves the target outlet and is split across 5 channels where readout later occurs upon mixing with the outlets from stage 2. Another inlet is present in this stage to inject a growth medium, Luria-Bertani (LB) broth, into the outlet channels and to help push bacteria along the filters [15].

Component	Size
Red blood cells (RBCs)	7.5-8.5µm
White blood Cells (WBCs)	7-20µm
Platelets	1.5-3µm
S. typhi	0.7-1.5µm by 2.0-5.0µm

Table 1. Size of components in blood

In stage 2 of our device, the linear concentration gradient is formed using a christmas tree system. The stage has two inlets: inlet A, which contains growth medium and resazurin dye for visualization after incubation and inlet B, which contains growth medium, dye, and antibiotic at the highest concentration of 32 mg/L [16]. These two inlet streams are driven at equal flow rate so mixing occurs at a 1:1 ratio. The tree geometry works by repeatedly splitting and recombining streams, so the concentration at each downstream node is simply the average of the two parent concentrations. Starting from 0 mg/L at Inlet A and 32 mg/L at Inlet B, the first split creates an intermediate node at 16 mg/L. Two more subsequent splits creates five final outlet concentrations: 0, 8, 16, 24, and 32 mg/L. These 5 antibiotic concentrations then mix with the 5 outlet channels containing bacteria from stage 1. The mixing junction now contains bacteria, antibiotic at respective concentration, growth medium, and resazurin. The device is then incubated at 37℃, allowing for visualization of bacteria viability and MIC determination [9].

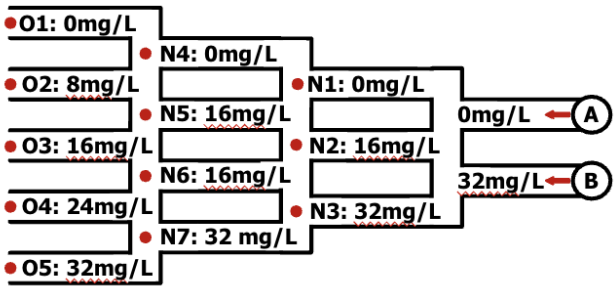

Figure 2: Concentrations of azithromycin in stage 2

However, to be able to visualize the bacterial growth, we must first determine the initial bacteria concentration needed in each of the five outlets at the end of stage 1 prior to incubation. To calculate this, we started with the model for exponential bacterial growth, $N = N_0 e^{\mu(t - t0)}$, where µ is the specific growth rate (1.28-1.95 h^{-1} for *S. Typhi*), N_0 is initial CFU/mL of S. Typhi at time $t=t_0$ [17, 18]. The standard bacterial suspension needed for fluorescent visualization is ~$5x10^5$ CFU/mL at readout [9, 19].

Plugging this value in for N, 1.95 for our growth rate, and 8 hours for incubation time, we get a reasonable starting bacteria concentration 0.08 CFU/mL. It should be noted that the specific growth rate could later be specified for our specific bacteria, growth medium, and incubation conditions via experimentally for more accurate results. This means that a concentration of at least 0.08 CFU/mL per outlet channel is needed prior to incubation to have sufficient bacteria suspension during readout, which is reasonable given that we are developing a point-of-care diagnostic where collecting large volumes of blood may not be feasible. This duration of 8 hours is longer than that used in other microfluidic methods, but shorter than the gold-standard and agar and broth dilution assays.

Given an estimated blood concentration of ~1 CFU/mL and a sample volume of 35 uL per drop of blood, each drop of blood contains on average 0.035 CFU per drop [20, 21]. It is important to acknowledge that for these calculations, we assume that bacteria is present at 1 CFU/mL everywhere in the blood and that each drop of blood contains bacteria. In practice, bacterial presence is highly variable at such low concentrations, but this assumption provides a conservative design estimate for finding the minimum channel volume. One drop of blood is then inserted into stage 1 of the device, ideally by a syringe pump. The bacteria filtered from the blood drop is then distributed evenly across the five parallel channels resulting in 0.035 CFU / 5 = 0.007 CFU per channel. Recalling that a concentration of 0.08 CFU/mL is needed in each channel, solving 0.007 CFU / x = 0.08 CFU/mL, gives us a required volume of ~87.5 µL per channel to ensure that the initial bacterial concentration is high enough for reliable detection following incubation. Since we wish to mix stage 1 and stage 2 at a 1:1 ratio, this corresponds to 43.75 µL of volume entering each channel from Stage 1 and 43.75 µL of volume entering each channel from Stage 2. We ensure these volumes by injecting around 220 µL of growth medium into stage 1's inlet and a total 220 µL of growth medium into inlet A and inlet B combined to result in around 43.75 µL into each of the five channels from each stage, resulting in a final volume of 87.5 µL in each channel.

For our Christmas tree, to achieve our desired concentrations, each mixing node combines two inlet streams at a 1:1 ratio, which requires the horizontal channels at each node to be symmetric in length. This is important because hydraulic resistance depends on channel length, and unequal resistances would cause uneven flow rates and incorrect concentration ratios in Stage 2 of our device [11]. Following the Christmas-tree design rationale, we enforce $R_V >> R_H$, where R_V and R_H are the resistances of the vertical (mixing) and the horizontal (splitting) channels. When this condition holds, horizontal channel resistance becomes negligible and flow splitting ratios are governed by the tree-branching topology rather than small fabrication variations [11]. Accordingly, vertical channels are designed to be five times longer than horizontal channels while maintaining constant width and height. This is later described further in the scaling considerations. Designing the channels this way ensures uniform flow rates across the outlets, which is necessary in mixing the bacteria and antibiotic flows in a 1:1 ratio, ensuring uniform exposure time across all outlets, and preventing shear stress on bacteria [11]. The lengths for the channel were then chosen as 500 µm for the horizontal channels and 2500 µm for the vertical channels. A width of 100 µm and a height of 25 µm were chosen for all the channels across stage 1 and stage 2. The flow rates were then calculated using the following: $Q_{in} = Q_{out}$, $Q_{inlet\ A\ +\ inlet\ B} = Q_{total\ outlet\ flow}$, where $Q_{total\ outlet\ flow} = Q_1 + ... + Q_5$. We set the flow rates using Q = V/T. Each outlet receives 43.75 uL over 10 minutes, corresponding to 4.375 uL/min per outlet. The total flow rate is 21.87 uL/min, split evenly between two inlets, giving 10.93 uL/min at inlet A and inlet B. The flow rate out of this stage 2 must equal the flow rate out of stage 1.

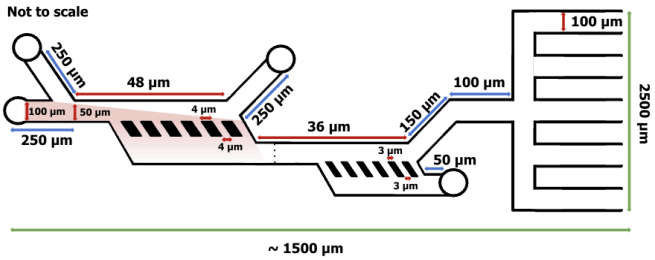

Figure 3: Dimensions of stage 1. Green arrows represent total dimensions and red arrows represent calculated dimensions. Blue arrows were dimension that were arbitrarily chosen.

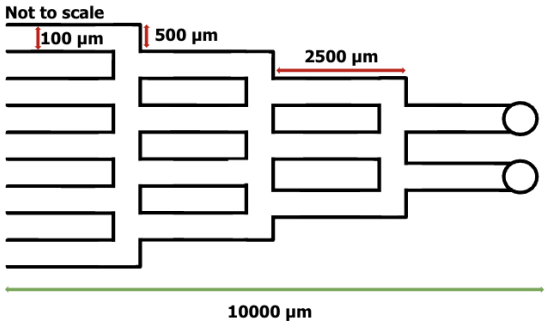

Figure 4: Dimensions of stage 2

Given this design constraint from stage 2, we finalize the design and dimensions for stage 1. If we include six pores evenly spaced in the platelet filtration region, the flow is distributed across multiple openings, which reduces the risk of clogging and limits local pressure buildup. The lengths of the main channel segments are chosen to be short in order to keep hydraulic resistance low while still allowing sufficient residence time for size-based separation. The width of the main channel is set to be at

least as large as the largest blood components (≥20 μm), but we increase it to approximately 100 μm to align with the geometry of Stage 2. The channel height is fixed at 25 μm to maintain laminar flow and fabrication consistency. To maintain flow balance, we enforce $Q_{in}=Q_{out}$, with each outlet set to 10.93 uL/min, giving a total flow rate of 32.79 uL/min, which is split evenly between the two inlets. Using these flow rates, the sample stream width is calculated as $b_0 = (Q_{sample})/(Q_{buffer} + Q_{sample})\ (w_{main})$, which gives a sample stream of approximately 50 μm in a 100 μm-wide channel [14]. These flow rates can be controlled using a syringe pump.

III. SCALING CONSIDERATIONS

For this device, the Navier-Stokes equation for an incompressible, Newtonian fluid governs the mechanisms for this device. To simplify our device, we assume that blood is a Newtonian, incompressible fluid [22, 23]. We also assume that at steady state, our flow is fully developed, laminar, and there are no edge effects. We therefore deduced the Navier Stokes equation for an incompressible, Newtonian fluid into the following:

$$\rho\frac{dv}{dt} + \rho v \cdot \nabla v = -\nabla p + \mu\nabla^2 v + \rho v + \sigma E$$

$$\rightarrow \frac{dP}{dx} = \frac{d\tau_{yx}}{dy}$$

This simplification can be used to find flow rate Q, which can then be used to find the hydrodynamic resistance for channels with non-square rectangular cross-sections:

$$R = \frac{12\eta L}{wh^3}\left(1 - 0.63\frac{h}{w}\right)^{-1}$$

This approximation for hydrodynamic resistance guided the dimensions for our device. In using this approximation, it must be held true that the width of our channels must be larger than the height of our device. This approximation also allowed us to create the vertical and horizontal channel lengths for the christmas tree gradient generator. An important consideration in achieving the concentrations needed for our device revolved around understanding how the hydraulic resistance scaled with channel length, as resistance directly controls flow rates in the network. Choosing the appropriate lengths and resistances allows us to achieve equal flow rates at the outlets and a linear concentration gradient, both of which are important in mixing the bacteria and antibiotic flows in a 1:1 ratio, ensuring uniform exposure time across all outlets, and minimizing shear stress on bacteria. Defining length scale as l, holding height (h) and width (w) constant throughout our device, and assuming that $L \propto l$, we find the following:

$$R = \frac{12\eta L}{wh^3}\left(1 - 0.63\frac{h}{w}\right)^{-1} \rightarrow R = \frac{12\eta l}{wh^3},\ R \propto l.$$

If $R \propto l$, then the resistance increases linearly with length. Therefore, we developed a similar approach to the christmas tree gradient generator created by Wang et. al [11], setting the resistances of the vertical channels to be five times greater than the resistances of the horizontal channels. To make the vertical channel resistance five times greater than the horizontal channel resistance, the vertical channels were made five times longer than the horizontal channels. Our dimensions were then finalized to be 2500 μM for the vertical channels and 500 μM for the horizontal channels.

IV. FABRICATION

The microfluidic device is fabricated using a soft lithography workflow to integrate a high-resolution bacterial separation stage with a downstream antibiotic concentration gradient generator (Figure 5). The design of the Stage 1 separation component is adapted from the cross-flow filtration principles described by Chiu et al., utilizing physical barriers to hydrodynamic focusing to separate larger blood components from smaller bacterial targets [14]. The Stage 2 component utilizes a symmetric tree network to generate linear antibiotic concentration gradients [11]. Both stages are fabricated in a single layer with a uniform height of 25 μm. The height was selected to balance the structural integrity of the high aspect ratio filtration pores with the need to minimize fluidic resistance for stable laminar flow, leveraging the high aspect ratio capabilities of the photoresist [24, 25].

The microfluidic features are patterned onto a 4 inch silicon wafer using SU-8 3025 negative photoresist (Kayaku Advanced Materials) to create the reusable template [25]. For the layer, the wafer is dehydrated at 200℃ and spin coated with SU-8 3025 at 3000 rpm to achieve the target height of 25 μm [25]. The layer is then soft baked on a hotplate at 95℃ for about 10 minutes. To resolve the smallest features, including the 3 μm and 4 μm pore features, which fall below the reliable resolution limit of standard transparency masks (about 10 μm), a chrome on glass photomask is utilized during UV exposure [26]. The exposure dose for this layer is set to 150-250 mJ/cm^2 [25]. A combined post exposure bake is performed so it is baked at 65℃ for 1 minute then 95℃ for about 3 minutes [25]. Then, a single development step in propylene glycol monomethyl ether acetate (PGMEA) dissolves the unexposed resist. The immersion development time is about 5 minutes [25].

The device is replicated using standard soft lithography. The template is silanized with trichloro silane vapor for 20 minutes. Polydimethylsiloxane (PDMS) is mixed at a 10:1 ratio (base:curing agent), degassed, and cured at 80℃ for 2 hours. Inlet and outlet pores are punched. The PDMS chips are bonded to glass slides using oxygen plasma treatment (50W for 45 seconds). To prevent non-specific bacterial adhesion and improve wetting, the channels are flushed with 1% Tween-20 prior to experimental use [27].

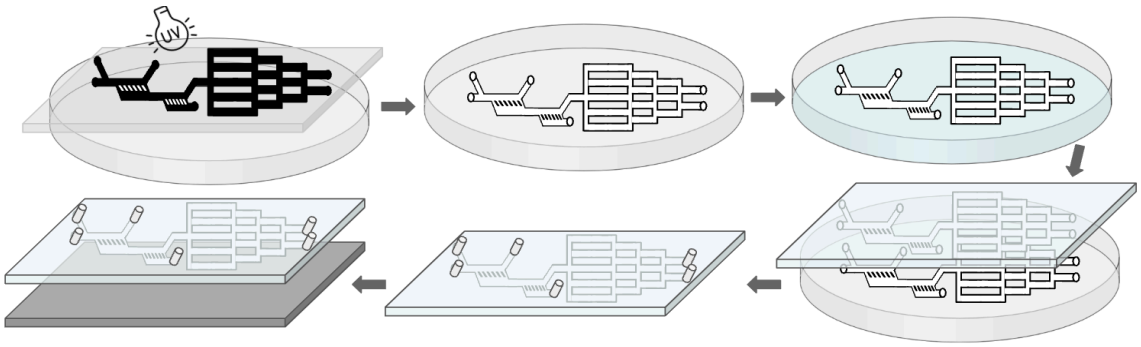

Figure 5: General fabrication steps of our device. Step 1 uses a SU-8 negative photoresist to make the master mold as seen in step 2. Steps of pouring PDMS, cutting, punching holes, and bonding to substrate then follows.

V. DISCUSSION

As previously mentioned, agar diffusion and broth microdilution are currently considered the modern methods for determining MIC of certain antibiotics. These processes, however, require 16-24 hours of incubation prior to readout. Our device combines a whole-blood bacterial separation stage with an antibiotic concentration gradient generator, enabling a total assay time of less than 9 hours. We recognize that there are other devices currently being researched that are able to achieve AST measurements for other bacterial cultures such as Escherichia coli in 4-5 hours [9]. Many of these devices, however, utilize urine or positive blood cultures as their sample source [9, 28]. By enabling bacterial isolation from a single drop of whole blood, our device provides an accessible testing method that supports rapid determination of appropriate antibiotic dosing. In addition, with our microfluidic device only requiring one drop of blood from a patient, we allow for point-of-care testing that can ideally screen larger patient populations and reduce unnecessary antibiotic dosing. In terms of fabrication, our device uses PDMS soft lithography materials, LB broth, resazurin dye, and possibly a syringe pump for better flow rate control of medium and blood sample into the device. LB broth typically costs around $40 for 1000mL and only 450 uL is needed per test, making this portion $0.018 per test [29]. Resazurin dye costs around $40 for 1 gram, but we expect to only use around 3 mg per test, making this portion around $0.12 per test [30, 31]. A typical soft lithography mask for SU-8 costs around $100, and a syringe pump on the microliter scale can cost around $350 [26, 32]. However, the syringe pump can be used for several tests and the soft lithography technique allows us to make several PDMS chips using the same SU-8 master mold. While the initial setup costs may be too expensive for widespread point-of-care testing, the low cost per-test may allow for more in-lab or in-clinic testing and offers a path toward creating more affordable point-of-care versions in the future. Further adjustments in creating a sample injection method that can achieve steady flow rates in the microliter scale may help reduce costs and improve feasibility for point-of-care applications.

VI. CONCLUSION

Our device gives a viable and necessary approach for rapid point of care antimicrobial resistance testing for *S. Typhi*. Our single layer microfluidic design utilizes whole blood separation followed by a symmetric tree gradient generator to determine the minimum inhibitory concentration of Azithromycin in under 9 hours which dramatically outperforms the 16-24 hours required by current clinical standards. The fast turnaround time is essential for administering effective and appropriate antibiotic dosage. This is important for controlling the spread of XDR typhoid fever. While the low cost materials offer great scalability for high volume manufacturing, a limitation is the system's reliance on a precision syringe pump for flow control. This needs to be addressed by future work by leveraging hydrostatic pressure and hand powered mechanisms. Experimental validation is also important to quantify bacterial loss through the 3 µm filtration stage. Overall, the design offers a path to an impactful accessible tool in low resource settings.

ACKNOWLEDGEMENTS

The authors would like to acknowledge Professor Streets and GSI Kevin Joslin for providing us with the knowledge and resources needed to complete this project.

REFERENCES

[1] Typhoid: A preventable global health threat [Internet]. Take on Typhoid; [cited 2025 Dec 17]. Available from: Typhoid: A preventable global health threat.

[2] Typhoid fever [Internet]. Mayo Clinic; c1998-2025 [updated 2025 Sept 16; cited 2025 Dec 17]. Available from: Typhoid fever.

[3] Muttiah B. From fever to action: diagnosis, treatment, and prevention of acute undifferentiated febrile illnesses. Pathog Dis. 2024 Apr 13;82:ftae006.

[4] Ullah A, Shabil M, Abdulsamad S, Jan A, Naeem A, Ullah H, Khattak M, Zakiullah. Prevalence of the Antibiotic Resistance of Salmonella typhi and Salmonella paratyphi in Pakistan: A Systematic Review and Meta-analysis. Open Forum Infectious Diseases 2025 Apr;12(4):ofaf131.

[5] Tanmoy A, Hooda Y, Sajib M, Rahman H, Sarkar A, Das D, Islam N, Kanon N, Rahman M, Garrett D, Endtz H, Luby S, Shahibdullah M, Amin M, Alam J, Hanif H, Saha S, Saha S. Trends in antimicrobial resistance amongst Salmonella Typhi in Bangladesh: A 24-year retrospective observational study (1999-2000). PLoS Negl Trop Dis. 2024 Oct;18(20):e0012558.
[6] Thirumoorthy T, Bakthavatchalam Y, Jacob J, Manoharan Y, John J, Rupali P, Walia K, Veeraraghavan B. Azithromycin resistance in Salmonella Typhi: navigating diagnostic uncertainties and clinical decision-making. JAC Antimicrob Resist. 2025 July;7(4):dlaf107.
[7] Bhandari J, Thada P, Hashmi M, DeVos E. Typhoid Fever [Internet]. StatPearls; c2025 [updated 2024 Apr 19; cited 2025 Dec 17]. Available from: Typhoid Fever.
[8] Watkins L, Shih D, Dorough L. Typhoid and Paratyphoid [Internet]. CDC; [updated 2025 Apr 23; cited 2025 Dec 17]. Available from: Typhoid and Paratyphoid Fever.
[9] Nguyen A, Yaghoobi M, Azizi M, Davaritouchaee M, Simpson K, Abbaspourrad A. Ladder-shaped microfluidic system for rapid antibiotic susceptibility testing. Nature Communications 2023 Apr 03;2(15).
[10] Fink G, Mitteramskogler T, Hintermüller M, Jakoby B, Wille R. Automatic Design of Microfluidic Gradient Generators. IEEE Access 2022 March 10;10.
[11]Wang Y, Ping C, Sun Y. Design of Christmas-Tree-like Microfluidic Gradient Generators for Cell-Based Studies. Chemosensors 2023;11(1): 2.
[12] Burkland A, Zhang J. Microfluidics-based organism isolation from whole blood - an emerging tool for bloodstream infection diagnosis. Ann Biomed Eng 2019 Apr;47(7):1657-1674.
[13] Salmonella Typhi [Internet]. Emory University; [cited 2025 Dec 17]. Available from: Salmonella Typhi
[14] Chiu Y, Huang C, Lu Y. Enhancement of microfluidic particle separation using cross-flow filters with hydrodynamic focusing. Biomicrofluidics 2016 Jan 21;10(1):011906.
[15] Day J, Basavanna U, Sharma S. Development of a Cell Culture Method To Isolate and Enrich Salmonella enterica Serotype Enteritidis from Shell Eggs for Subsequent Detection by Real-Time PCR. Appl Environ Microbiol. 2009;75.
[16] Kowalska-Krochmal Beata, Dudek-Wicher R. The Minimum Inhibitory Concentration of Antibiotics: Methods, Interpretation, Clinical Relevance. Pathogens 2021 Feb 4;10(2):165.
[17] Arana I, Orruno M, Barcina I. How to Solve Practical Aspects of Microbiology [Internet]. [updated 2013; cited 2025 Dec 17]. Available from: HOW TO SOLVE PRACTICAL ASPECTS OF MICROBIOLOGY.
[18] Silva R, Moraes C, Bessan J, Vanetti M. Validation of a predictive model describing growth of Salmonella in enteral feeds. Braz J Microbiol. 2009 Mar 1;40(1):149-154.
[19] Smith K, Kirby J. The Inoculum Effect in the Era of Multidrug Resistance: Minor Differences in Inoculum Have Dramatic Effect on MIC Determination. Antimicrob Agents Chemother. 2018 Jul 27;62(8):e00433-18.
[20] Wain J, Diep T, Ho V, Walsh A, Nguyen T, Parry C, White N. Quantitation of bacteria in blood of typhoid fever patients and relationship between counts and clinical features, transmissibility, and antibiotic resistance. J Clin Microbiol. 1998 Jun;36(6):1683-7.
[21] Not Every Drop of Blood is Identical [Internet]. Biomedical Engineering, The Partnership for Global Health Technologies; [updated 2016 Mar 21; cited 2025 Dec 17]. Available from: Not Every Drop of Blood Is Identical.
[22] Sugawara M. Blood Flow in the Aorta. Springer Tokyo. 1989.
[23] Nader E, Skinner S, Romana M, Fort R, Lemonne N, Guillot N, Gauthier A, Antoine-Jonville S, Renoux C, Hardy-Dessources M, Stauffer E, Joly Pm Bertrand Y, Connes P. Blood Rheology: Key Parameters, Impact on Blood Flow, Role in Sickle Cell Disease and Effects of Exercise. Front. Physiol. 2019 Oct 16;10.
[24] Beebe D, Mensing G, Walker G. Physics and Applications of Microfluidics in Biology. Annual Review of Biomedical Engineering 2002 Feb;4(1):261-86.
[25] SU-8 Series [Internet]. Kayaku Advanced Materials; c2025 [cited 2025 Dec 17]. Available from: SU-8 3000.
[26] SU-8 photolithography: photomask [Internet]. Elve Flow; c2025 [cited 2025 Dec 17]. Available from: SU-8 photolithography: photomask.
[27] Wu C, Lim J, Fuller G, Cegelski L. Disruption of E. coli amyloid-integrated biofilm formation at the air-liquid interface by a polysorbate surfactant. Langmuir 2013 Jan 9;29(3):920-926.
[28] Khanal P, Richardson J, Richardson K, Damhorst G, Oertell O, Filbrun A, Burd E, Dickson R. Rapid colorimetric antimicrobial susceptibilities direct from positive blood culture for Gram-negative bacteria. Microbiol Spectr. 2025 Nov 4;13(11):e0214725.
[29] LB Broth [Internet]. Sigma Aldrich; c2025 [cited 2025 Dec 17]. Available from: LB Broth (Miller).
[30] Resazurin sodium salt [Internet]. Sigma Aldrich; c2025 [cited 2025 Dec 17]. Available from: Resazurin sodium salt.
[31] Carvalho N, Sato D, Pavan F, Ferrazoli L, Chimara E. Resazurin Microtiter Assay for Clarithromycin Susceptibility Testing of Clinical Isolates of Mycobacterium abscessus Group. Journal of Clinical Laboratory Analysis, 206;30:751-755.
[32]InfusionONE Single Channel Syringe Pump [Internet]. United States Plastic Corp; c2000-2025 [cited 2025 Dec 17]. Available from: InfusionONE Single Channel Syringe Pump.